Amyloid Precursor-like Protein 1 Influences Endocytosis and Proteolytic Processing of the Amyloid Precursor Protein[*]

Stephanie Neumann[‡]**, Susanne Schöbel**[‡]**, Sebastian Jäger**[§]**, Anna Trautwein**[§]**, Christian Haass**[‡]**, Claus U. Pietrzik**[§]**, and Stefan F. Lichtenthaler**[‡1]

From the [‡]*Adolf-Butenandt-Institut, Ludwig-Maximilians-University, Schillerstrasse 44, 80336 Munich and the* [§]*Institute of Physiological Chemistry and Pathobiochemistry, University of Mainz, Duesbergweg 6, 55128 Mainz, Germany*

Ectodomain shedding of the amyloid precursor protein (APP) is a key regulatory step in the generation of the Alzheimer disease amyloid β peptide (Aβ). The molecular mechanisms underlying the control of APP shedding remain little understood but are in part dependent on the low density lipoprotein receptor-related protein (LRP), which is involved in APP endocytosis. Here, we show that the APP homolog APLP1 (amyloid precursor-like protein 1) influences APP shedding. In human embryonic kidney 293 cells expression of APLP1 strongly activated APP shedding by α-secretase and slightly reduced β-secretase cleavage. As revealed by domain deletion analysis, the increase in APP shedding required the NPTY amino acid motif within the cytoplasmic domain of APLP1. This motif is conserved in APP and is essential for the endocytosis of APP and APLP1. Unrelated membrane proteins containing similar endocytic motifs did not affect APP shedding, showing that the increase in APP shedding was specific to APLP1. In LRP-deficient cells APLP1 no longer induced APP shedding, suggesting that in wild-type cells APLP1 interferes with the LRP-dependent endocytosis of APP and thereby increases APP α-cleavage. In fact, an antibody uptake assay revealed that expression of APLP1 reduced the rate of APP endocytosis. In summary, our study provides a novel mechanism for APP shedding, in which APLP1 affects the endocytosis of APP and makes more APP available for α-secretase cleavage.

The amyloid precursor protein (APP)[2] is one of a large number of membrane proteins that are proteolytically converted to their soluble counterparts. This process is referred to as ectodomain shedding and is an important way of regulating the biological activity of membrane proteins (1, 2). The shedding of APP may occur through two different protease activities termed α- and β-secretase, which cleave APP within its ectodomain close to its transmembrane domain (for a review, see Ref.

3) (see Fig. 1*A*). APP cleavage by α- or β-secretase is a key regulatory process in the generation of the amyloid β peptide (Aβ). Generation and subsequent deposition of Aβ are assumed to be the first events in the pathogenesis of Alzheimer disease. β-Secretase has been identified as the aspartyl protease BACE1 and cleaves APP at the N terminus of the Aβ peptide domain, thus catalyzing the first step in Aβ peptide generation (4). After the initial cleavage of APP by BACE1, the remaining C-terminal APP fragment is cleaved by γ-secretase within its transmembrane domain at the C terminus of the Aβ domain, leading to the secretion of the Aβ peptide (5). In contrast to β-secretase, α-secretase cleaves within the Aβ sequence and thereby precludes the generation of the Aβ peptide. α-Secretase is a member of the ADAM family of proteases. Candidate α-secretases are ADAM10, ADAM17 (TACE), or ADAM9 (6). α-Secretase cleavage of APP is assumed to take place at or close to the cell surface, whereas β-secretase cleavage takes place after endocytosis of wild-type APP into endosomes. Endocytosis of APP requires the cytoplasmic amino acid motif NPTY, which belongs to the NP*XY* class of endocytic motifs found in a small number of type I membrane proteins (7), including the two mammalian APP homologs APLP1 and APLP2 (amyloid precursor-like protein 1 and 2). Like APP, APLP2 is ubiquitously expressed, whereas expression of APLP1 is strongest in brain (for an overview, see Ref. 8). Both proteins undergo protease cleavage events similar to those of APP (9–12). Whether the three APP family members can mutually affect their proteolytic processing is unknown. Despite a high degree of similarity to APP, APLP1 and APLP2 lack the Aβ peptide domain. However, both proteins have been found in the amyloid plaques in the brain of Alzheimer patients (13) and thus may potentially contribute to the pathogenesis.

Although the ectodomain shedding of APP by α- or β-secretase has opposite effects on Aβ generation, little is known about the molecular mechanisms that control to what extent APP shedding occurs by either protease. Different kinases, including protein kinase C, mitogen-activated protein kinases, and protein kinase A, can stimulate APP α-cleavage, but downstream molecular target proteins remain to be identified (6). Additionally, cytoplasmic adapter proteins, such as FE65, have been reported to bind to the cytoplasmic domain of APP and to alter APP shedding (for reviews, see Refs. 14 and 15). The FE65 family of cytoplasmic multidomain adapter proteins consists of three family members, FE65, FE65L1, and FE65L2 (for a review, see 15). FE65 colocalizes with APP in actin-rich lamellipodia in neuronal growth cones (16) and may link APP to cellular motility (17). Moreover, it may be involved in the potential transcriptional regulation of the γ-secretase-cleaved APP intracellular domain (18, 19). According to a recently suggested model, FE65 links APP to the low density lipoprotein receptor-related protein (LRP), which is a multifunctional cell surface receptor for proteins involved in lipoprotein metabolism (20) and which modulates APP processing and Aβ generation (21, 22). The complex of APP, FE65, and LRP seems to be required for efficient endocytosis of APP (23–25). In

contrast, in cells lacking LRP, APP endocytosis was reduced (22). As a consequence, APP β-cleavage in the endosomes was also reduced, and APP α-cleavage was increased (21, 22).

In this study we identified APLP1 as a novel activator of APP α-cleavage. This activation required the endocytic GYENPTY motif in the cytoplasmic domain of APLP1. Concerning the underlying molecular mechanism, we show that APLP1 reduces APP endocytosis and that the increase in APP shedding occurs in an LRP-dependent manner. Thus, our study provides further evidence for a complex of LRP with APP which controls APP endocytosis and shedding.

EXPERIMENTAL PROCEDURES

Reagents—The following antibodies were used: anti-HA epitope antibody HA.11 (Covance), anti-FLAG (Sigma), horseradish peroxidase-conjugated goat anti-mouse secondary antibody (DAKO), anti-insulin receptor (IR) (BD Transduction Laboratories), anti-EGFR (BD Transduction Laboratories), anti-EEA1 (BD Transduction Laboratories), horseradish peroxidase-coupled goat anti-mouse (DAKO), horseradish peroxidase-coupled goat anti-human IgG Fc (Cappel), Alexa 555-coupled secondary anti-rabbit and Alexa 488-coupled secondary anti-mouse (Molecular Probes). Antibodies 5313 (against APP ectodomain) and 6687 (against APP C terminus) were described previously (26). Monoclonal antibodies 1G7, 5A3 (against APP ectodomain) as well as LRP1704 against the LRP C terminus were described (22). Antibody 192wt specific for the C terminus of APPsβ (27) was provided by Dale Schenk. Antibodies 22C11 (anti-APP ectodomain), W02 (against amino acids 5–8 of Aβ) (28), Ab150 (against Aβ-like domain of APLP1) (10), Ab57 (against C terminus of APLP1) were provided by Simone Eggert and Konrad Beyreuther. The specific γ-secretase inhibitor DAPT was provided by Boris Schmidt (University of Darmstadt, Germany).

Plasmid Construction—Generation of vector peak12 expressing human BACE1 and ADAM10 has been described (29). The cDNA of human APLP1 in the peak8 expression vector was obtained from a human brain cDNA library (Edgebio). The human cDNAs of BACE1 (1503-nucleotide open reading frame), APP (2085-nucleotide open reading frame), APLP1 (1950-nucleotide open reading frame), and APLP2 (2253-nucleotide open reading frame) tagged with a C-terminal HA epitope tag were cloned into the expression vector peak12. Likewise, human L-selectin (without its signal peptide; starting at nucleotide 154 of the open reading frame) carrying an N-terminal HA epitope tag and the signal peptide of CD5 was cloned into peak12. Rat dynamin 1 K44A was amplified from plasmid pCB1/dynamin1 K44A (obtained from Marc Caron) and cloned into the peak12 vector together with a C-terminal HA tag. Plasmid pRK5-hIR encoding the human insulin receptor was obtained from Axel Ullrich. Plasmid pcDNA3/EGFR was obtained from Gordon Gill. The plasmids pCEP4/APLP1, pCEP4/APLP1ΔNPTY (carrying an N-terminal myc tag and lacking the cytoplasmic GYENPTY amino acid motif) and pCEP4/APLP2 were obtained from Simone Eggert and Konrad Beyreuther (10). The intracellular domains of human APLP1 (starting with nucleotide A1813 of the coding region) and TACE (starting with nucleotide G2083 of the coding region) were amplified by PCR, digested with MluI/NotI, and ligated into the peak12 expression vector (digested with HindIII/NotI) together with the sIg7 HindIII/MluI fragment derived from vector cdm12/sIg7 (obtained from Brian Seed). The resulting plasmids encode fusion proteins consisting of the human IgG1 constant region as ectodomain (secreted Ig, sIg), followed by the transmembrane domain of CD7 and the cytoplasmic domain of the indicated proteins. The cDNA of TACE was amplified by PCR from an activated T cell library.

The peak12 vectors encoding the C-terminal fragments (CTF) of APLP1 (ectodomain deletion constructs) consist of the signal peptide of CD5 followed by an HA epitope tag and the C-terminal 106 amino acids of APLP1 (starting with residues QYERK). CTF106Δcyto has a deletion of the 42 cytoplasmic amino acids and stops after the membrane anchor sequence RRKKP. CTF106ER has an ER retention signal of the KKXX-type added to the C terminus of APLP1 (. . . EERPGKKQN). Peak12/GFP-ICD encodes a fusion protein consisting of GFP fused to the N terminus of the 50 C-terminal amino acids of APLP1 (starting with LLLRRKKP, corresponding to an ϵ-cleavage-like fragment). Plasmid peak12/sIg7-APLP1(Y/S) has tyrosine 638 mutated to serine. Plasmid pcIneo/LRP-CT (C-terminal fragment of LRP) was generated by subcloning the sequence that encodes for the C-terminal 370 amino acids of the LRP β-subunit together with a signal peptide from the LRP-CT/pBabehygro vector (22) into the EcoRI and NotI sites of the pcIneo vector (Promega). Plasmid pcDNA3/FE65-FLAG (C-terminal FLAG tag) was described previously (24). The identity of all constructs obtained by PCR was confirmed by DNA sequencing.

Cell Culture, Transfections, Western Blot—Human embryonic kidney 293-EBNA cells (HEK293) cells were cultured in Dulbecco's modified Eagle's medium (Invitrogen) containing 10% fetal bovine serum (Hyclone), 50 units/ml penicillin, and 50 μg/ml streptomycin. Clonal HEK293 cells expressing AP-APP and Bcl-X$_L$/CrmA were generated and cultured as described previously (29). Transfections were carried out using Lipofectamine 2000 (Invitrogen). One day after transfection, the medium was replaced with fresh medium. After overnight incubation the conditioned medium and the cell lysate (in 50 mM Tris, pH 7.5, 150 mM NaCl, 1% Nonidet P-40) were collected. For AP measurements, aliquots of the conditioned medium were treated for 30 min at 65 °C to heat inactivate the endogenous AP activity. AP activity was measured in the conditioned medium and the cell lysate as described previously (29) and corrected for the protein concentration in the cell lysate.

To detect secreted and cellular APP or other cellular proteins, the protein concentration in the cell lysate was measured, and corresponding aliquots of lysate or conditioned medium were loaded directly onto an electrophoresis gel. Western blot detection was carried out using the indicated antibodies. HEK293 cells stably expressing APLP1 and BACE1 were generated using plasmids peak8/APLP1 and peak12/BACE1-HA, respectively, using 0.5 μg/ml puromycin (Sigma). LRP-deficient Chinese hamster ovary (CHO) cell line (13-5-1) and corresponding LRP-expressing CHO K1 control cells (kind gift from Dr. S. Leppla, National Institutes of Health, Bethesda, MD), were grown in α-Dulbecco's modified Eagle's medium supplemented with 10% fetal bovine serum (24). CHO cells were transiently transfected with APLP1 and LRP-CT using Lipofectamine 2000.

Inhibition of γ-Secretase—HEK293 cells were transiently transfected with APLP1 or as a control with empty vector. Two days after transfection the cells were preincubated for 45 min in the presence of the inhibitor and then incubated for an additional 8 h with fresh medium containing the inhibitor. The specific γ-secretase inhibitor DAPT (1 μM) (30) was dissolved in dimethyl sulfoxide. Control cells were treated with dimethyl sulfoxide alone. Aliquots of the cell lysate were analyzed by Western blotting. For the detection of the APLP1 C-terminal fragments the lysate was immunoprecipitated with antibody Ab57 against the C terminus of APLP1.

FE65 Coimmunoprecipitation—HEK293 cells were transiently cotransfected with FE65 and APP, the IR, wild-type and mutant APLP1, with sIg7-APLP1 constructs or as a control with empty vector. Two days after transfection the cells were lysed in 50 mM Tris, pH 7.5, 150 mM NaCl, 1% Nonidet P-40. After preclearing cell lysates were incubated for
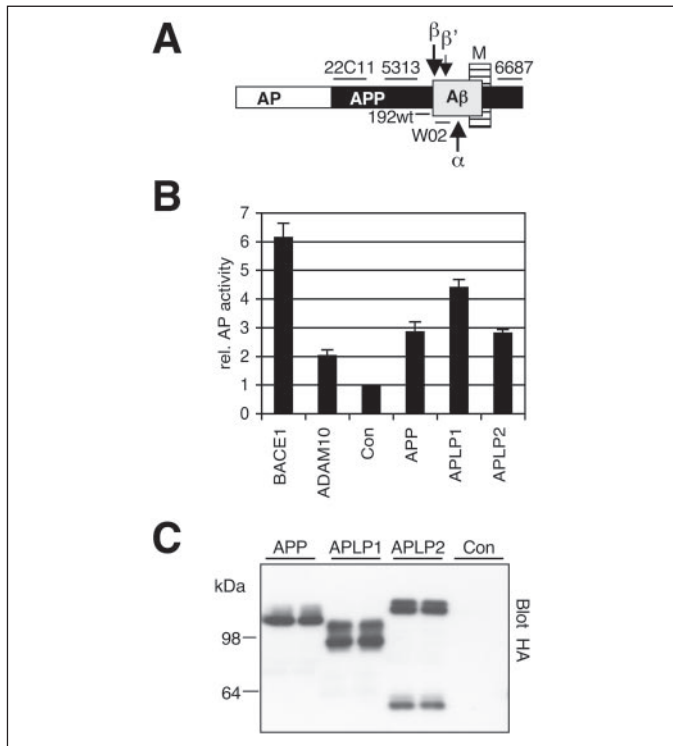
FIGURE 1. **APLP1 stimulates the shedding of an AP-APP reporter protein.** *A*, schematic drawing of the AP-APP fusion protein. The AP ectodomain was fused to the N terminus of full-length APP695 lacking its signal peptide. *Horizontal bars* show the epitopes recognized by the indicated antibodies. *Arrows* indicate the proteolytic α-, β-, and β'-cleavage sites within the APP ectodomain. The β'-cleavage site is an additional cleavage site of the β-secretase BACE1. *M*, membrane. *B* and *C*, HEK293 cells stably expressing AP-APP were transiently transfected with plasmids encoding the indicated cDNAs. AP activity was measured in the conditioned medium relative to the control (*Con*) transfected cells (*B*). Aliquots of the cell lysate were blotted for expression of the transfected APP, APLP1, and APLP2 using an antibody against their C-terminal HA epitope tag (*C*, from duplicate transfections). The AP activity represents the mean of two independent experiments, each one carried out in duplicate.

2 h with a 1:100 diluted anti-FLAG antibody and protein G-Sepharose or with protein G-Sepharose alone (for precipitation of sIg7-APLP1 constructs). After washing of the beads bound proteins were separated by electrophoresis and detected by immunoblot analysis with the indicated antibodies.

APP Antibody Uptake Assay—COS cells plated on coverslips were cotransfected with wild-type APP695 and C-terminally GFP-tagged APLP1 or GFP as a control. APP endocytosis was determined as described previously (31). In brief, transfected COS cells were washed in ice-cold PCM (phosphate-buffered saline supplemented with 1 mM $CaCl_2$, 0.5 mM $MgCl_2$), and incubated on ice in a 1:200 dilution of antibody 5313 in PCM. After 20 min, cells were washed in PCM on ice, and then PCM was replaced by prewarmed culture medium, and cells were placed in a 37 °C incubator. After the indicated time points, coverslips were transferred to 4% paraformaldehyde, 4% sucrose in phosphate-buffered saline, fixed for 20 min, and processed for standard immunofluorescence using 1:500 diluted Alexa 555-coupled secondary anti-rabbit antibodies or 1:100 diluted EEA1 antibody followed by 1:500 diluted Alexa 488-coupled secondary anti-mouse antibodies. Fixed cells were analyzed on a Zeiss Axioskop2 plus microscope equipped with a 63×/ 1.25 objective and standard FITC and TRITC fluorescence filter sets. Images were obtained using a Spot Camera (Zeiss AxioCam HRm) and the MetaView Imaging software (Universal Imaging Corp.). APP and EEA1 costainings were analyzed using a Zeiss 510Meta confocal system
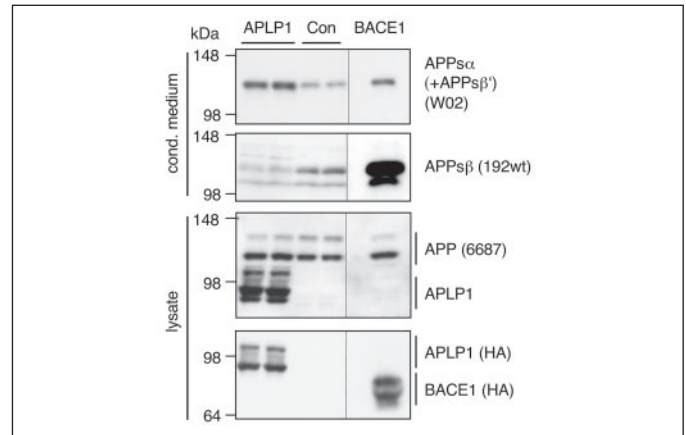

FIGURE 2. **APLP1 stimulates the α-secretase cleavage of the endogenous APP of 293 cells.** HEK293 cells were transiently transfected with APLP1, BACE1, or control vector (*Con*). Aliquots of the conditioned medium and the cell lysate were loaded directly onto electrophoresis gels. By immunoblot analysis APP secreted into the conditioned medium (*top panels*) or APP in the cell lysate (*middle panel*) were detected using antibodies W02 (detecting soluble APP cleaved at the α- or β'- site, APPsα, APPsβ'), 192wt (detecting the β-cleaved soluble APP, APPsβ), or 6687 (binding to the C terminus of full-length APP), respectively. Antibody 6687 also detects the transfected APLP1. Expression of APLP1 and BACE1 was detected using an antibody against their C-terminal HA epitope tag. Shown are representative blots of two independent experiments. The *vertical lines* on the blots indicate that the samples were loaded on the same gel, but not directly next to each other.

equipped with an 100/1.3 objective. Experiments were performed at least three times and were carried out under double blind conditions. At time point 0 min all cells showed cell surface APP staining. At time points 7 min, 20 min, and 35 min some cells started undergoing endocytosis, whereas other cells had not yet started. Thus, around 100 cells were scored/cell line and time point. Statistical significance was determined with Student's *t* test.

RESULTS

APLP1 Stimulates the Shedding of APP—For the rapid detection of APP shedding we used the following reporter cell line. HEK293 cells were stably transfected with a cDNA expression vector encoding a fusion protein (AP-APP) consisting of secretory alkaline phosphatase (AP) upstream from full-length APP (Fig. 1*A*) (29). The expression level of AP-APP in this cell line is similar to the expression level of the endogenous APP (32). In an expression cloning approach, cDNAs from a human brain cDNA library were transfected into the AP-APP cell line and screened for activators of APP shedding. This way we identified the cDNA of APLP1 as a stimulator of APP shedding. Transfection of APLP1 into the AP-APP expressing cells resulted in a strong increase in AP-APP shedding compared with control vector transfected cells (>4-fold, Fig. 1*B*). Because APLP1 is a member of the APP gene family comprising APP, APLP1, and APLP2, we tested whether APP and APLP2 could also stimulate shedding in the AP-APP reporter cell line. Both APP and APLP2 stimulated APP shedding, although not as strongly as APLP1 (Fig. 1*B*). All three proteins were expressed at similar levels, as detected by immunoblotting of the cell lysates using an antibody against their C-terminal HA epitope tag (Fig. 1*C*). As a control, transfection of the β-secretase BACE1 strongly increased APP shedding (6-fold; Fig. 1*B*). Transfection of the α-secretase ADAM10 led to a moderate increase in APP shedding (2-fold), which is in agreement with a previous publication (29). Next, we tested the effect of APLP1 on APP shedding in HEK293 cells expressing the endogenous wild-type APP that is not fused to the AP reporter. To this aim, HEK293 cells were transiently transfected with APLP1, BACE1, or control vector. Soluble APP generated by α-secretase (APPsα) or by β-secretase (APPsβ) was detected in
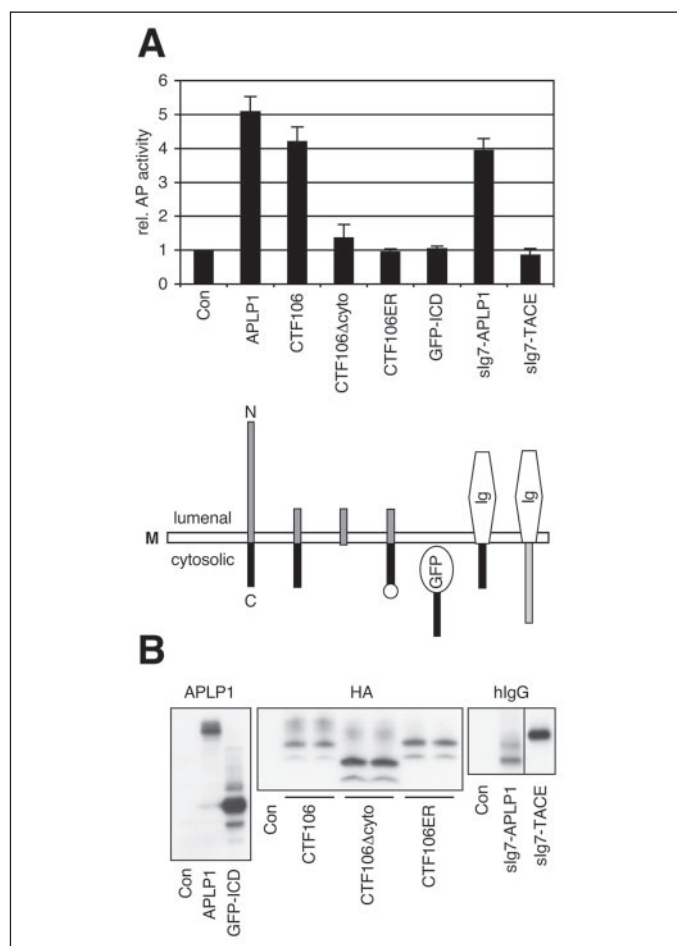
FIGURE 3. **Domain deletion analysis of APLP1.** The indicated APLP1 mutants were transiently transfected into AP-APP cells. *A*, AP activity was measured in the conditioned medium relative to the control cells and represents the mean ± S.D. of two independent experiments, each one carried out in duplicate. A schematic drawing of the mutants is given below the AP diagram. The N and C termini of APLP1 are indicated (*N, C*) as well as the membrane (*M*) and the luminal and the cytosolic sides of the membrane. *B*, aliquots of the cell lysate were blotted for expression of the transfected constructs using antibodies against APLP1 (Ab57), the N-terminal HA epitope tag (shown in duplicate transfections), or human IgG1 (hIgG). The CTF106 proteins are visible as a major protein band and a minor one of a lower molecular mass, which may result from C-terminal truncation of the protein. The *vertical line* on the *right panel* indicates that the two lanes were on the same gel but not directly next each other. *CTF106*, C-terminal fragment comprising C-terminal 106 amino acids of APLP1; *CTF106Δcyto*, CTF106 lacking the cytoplasmic domain; *CTF106ER*, CTF106 with an ER retention signal; *GFP-ICD*, fusion protein of GFP and the intracellular domain of APLP1; *sIg7-APLP1/TACE*, chimeric type I membrane protein consisting of the human IgG1 constant region as the ectodomain, followed by the transmembrane domain of CD7, followed by the intracellular domain of APLP1 or TACE.

the conditioned medium using cleavage site-specific antibodies. Antibody 192wt specifically detects APPsβ (27), whereas antibody W02 binds to an epitope between the β- and the α-secretase cleavage sites (28). Therefore, W02 does not detect APPsβ, but instead APPsα and APPsβ′, which starts at residue Glu-11 of the Aβ sequence and represents a minor secondary cleavage site of BACE1 (Fig. 1A). Compared with control cells W02 detected a strong increase in soluble APP in the APLP1-expressing cells (Fig. 2). Antibody 192wt detected a mild decrease in soluble APP, which was not always seen. This reveals that APLP1 stimulates the α-secretase cleavage of APP, but only has a mild effect on β-cleavage. As a control, BACE1-expressing cells showed a strong increase in APPsβ secretion detected by antibody 192wt (Fig. 2, 192wt blot). Antibody W02 also detected an increase in soluble APP in BACE1-transfected cells. This increase was much less pronounced than the one detected with 192wt and is likely to result from APPsβ′ generation, but not from APPsα. Expression of APLP1 and BACE1 did not
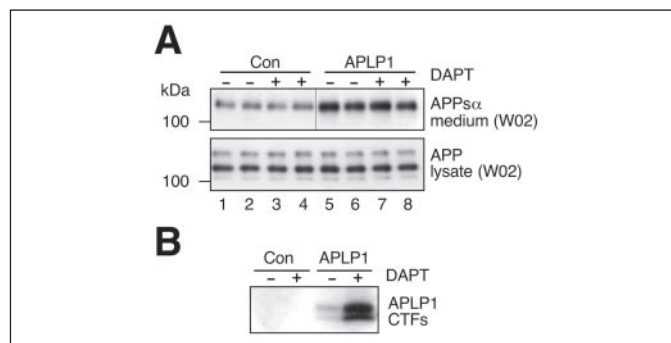

FIGURE 4. **APLP1-induced APP shedding is independent of γ-secretase activity.** HEK293 cells expressing endogenous APP were transiently transfected with control vector (*Con*) or APLP1 plasmid and treated for 8 h with dimethyl sulfoxide as a control or with the specific γ-secretase inhibitor DAPT. *A*, aliquots of the conditioned medium and the cell lysate were separated by electrophoresis and blotted for soluble APP in the conditioned medium or total APP in the cell lysate using antibody W02. The *vertical bar* on the *upper panel* indicates that the control and the APLP1 samples were on the same gel, but not directly next to each other. *Lanes* are *numbered* below the *panels*. *B*, cell lysates were blotted for C-terminal fragments of APLP1 (*APLP1 CTFs*), which are visible in the APLP1-transfected but not in the control transfected cells. The γ-secretase inhibitor DAPT increases the amount of CTFs.

alter the total amount of full-length APP in the cell lysate, as determined using an antibody against the C terminus of APP (Fig. 2). APLP1 and BACE1 were detected in the cell lysate with an antibody against their C-terminal HA epitope tag. Similar results were obtained in HEK293 cells stably transfected with BACE1 or APLP1 (data not shown). Interestingly, the APLP1-induced increase in APP shedding was only observed in HEK293 cells expressing low levels of APP, such as the endogenous APP (Fig. 2) or the AP-APP (Fig. 1B), which is expressed at levels similar to the endogenous APP (32). In contrast, in HEK293 cells stably transfected with APP the increased APP shedding was not seen, but instead an increased amount of mature APP was visible (data not shown).

Domain Deletion Analysis of APLP1—To start analyzing the mechanism by which APLP1 increases APP shedding, we carried out a domain deletion analysis and determined which APLP1 domains were required for the shedding-inducing effect. APLP1 and the deletion mutants were transiently transfected into the AP-APP reporter cell line. Mutant construct CTF106 (Fig. 3A) is a C-terminal fragment of APLP1 and roughly corresponds to the C99 fragment of APP. CTF106 consists of the C-terminal 106 amino acids of APLP1 and thus comprises a short fragment of the ectodomain, the transmembrane domain and the cytoplasmic domain of APLP1. CTF106 still increased APP shedding (Fig. 3A), revealing that most of the ectodomain is not required for the increase in APP shedding. In contrast, CTF106 lacking the cytoplasmic domain (CTF106Δcyto) had lost its ability to induce APP shedding, revealing an essential role for the cytoplasmic domain in stimulating APP shedding. Likewise, transfection of the APP C99 fragment increased APP secretion, but APP C99 lacking its cytoplasmic domain did not (data not shown). Addition of an ER retention motif to the C terminus of the APLP1 CTF106 abolished the APP shedding effect (Fig. 3A), demonstrating that CTF106 needs to be transported out of early cellular secretory compartments to increase APP shedding. Additionally, the cytoplasmic domain of APLP1 needs to be membrane-anchored to induce APP shedding. The cytoplasmic domain of APLP1 had no effect on APP shedding when fused to the soluble cytoplasmic protein GFP (GFP-ICD, Fig. 3A). In contrast, it strongly activated APP shedding when fused to a chimeric type I membrane protein comprising the human IgG1 constant region as ectodomain, followed by the CD7 transmembrane domain (sIg7; fusion protein sIg7-APLP1; Fig. 3A). To ensure that the sIg7 fusion part did not affect APP shedding, an additional protein was

FIGURE 5. **The cytoplasmic GYENPTY motif is required for the APLP1-induced increase in APP shedding.** AP-APP cells were transfected with the indicated cDNAs. *A*, AP activity was measured in the conditioned medium relative to the control (*Con*) cells and represents the mean ± S.D. of two independent experiments, each one carried out in duplicate. *APLP1ΔNPTY*, APLP1 lacking the cytoplasmic amino acid motif GYENPTY. *B*, experiments carried out as in *A*. *C*, cell lysates were separated and blotted for the indicated cDNAs. The *asterisk* denotes the endogenous LRP β. *IR fl.*, IR full-length. *D*, alignment of the NP*XY* amino acid motif of APP, APLP1, the IR, and LRP. LRP has two NP*XY* motifs denoted with *(1)* and *(2)*, only LRP *(2)* binds FE65. The *numbers* on the *left* indicate the numbers of amino acids between the end of the transmembrane domain (*Tm*) and the start of the NP*XY* motif. The *numbers* on the *right* indicate the numbers of amino acids C-terminal to the NP*XY* motif before the C-terminal end of the protein (modified after Ref. 7). *E, left panel*, experiments carried out as in *A*. *sIg7-APLP1 (Y/S)*, Tyr-638 is mutated to Ser. *Right panel*, cell lysates were separated and blotted for the indicated expressed cDNAs.
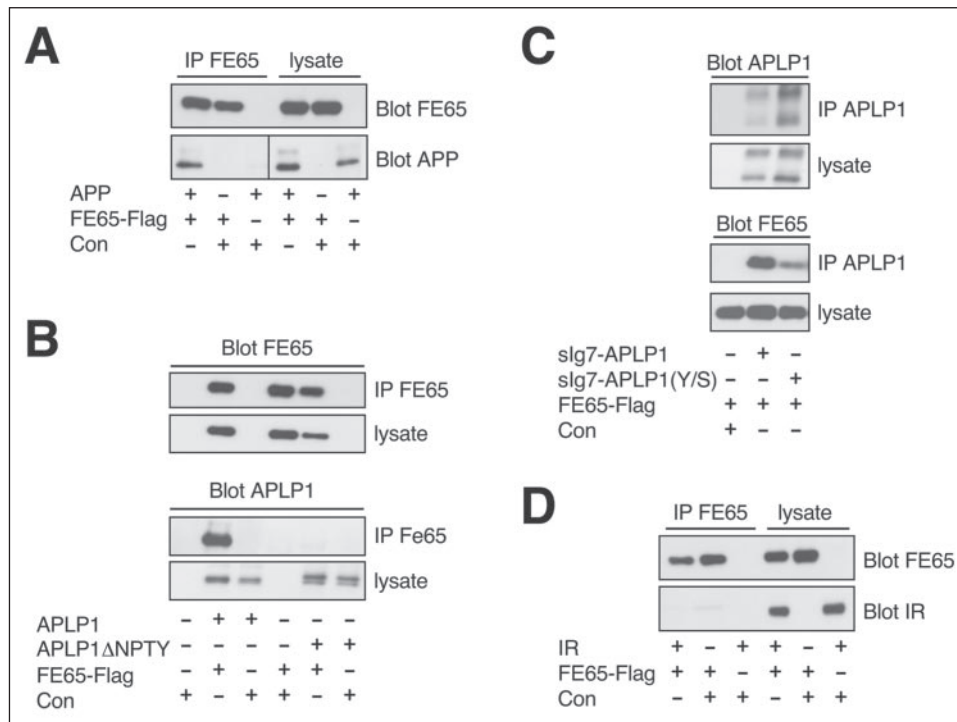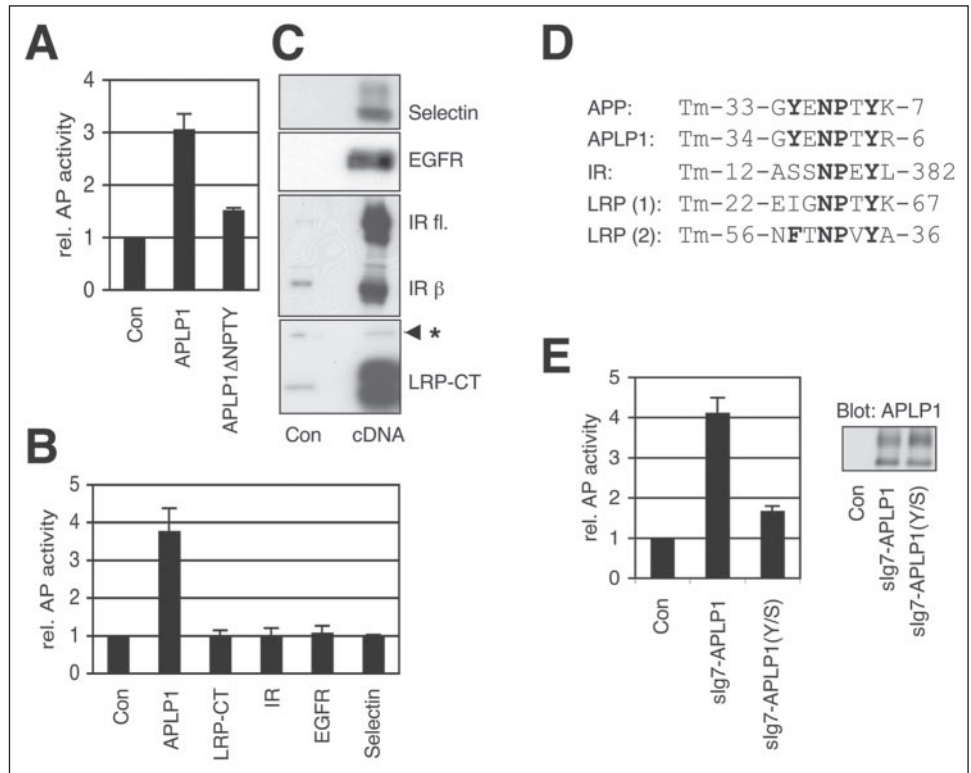

FIGURE 6. **The cytoplasmic GYENPTY motif is necessary for binding of APLP1 to FE65.** HEK293 cells were transiently cotransfected with FLAG-tagged FE65 and additionally APP, APLP1, mutants of APLP1 (APLP1ΔNPTY, sIg7-APLP1, sIg7-APLP1(Y/S)), the IR, or as a control (*Con*) empty vector. Cell lysates were immunoprecipitated with anti-FLAG antibody (*A*, *B*, and *D*) or with protein G-Sepharose alone (*C*, directly binding the Ig part of the sIg7 proteins). Immunoprecipitated proteins were analyzed by gel electrophoresis and immunoblot using the indicated antibodies. For every immunoprecipitation two immunoblots are shown, one for the precipitated protein (*e.g.* FE65 in *A*) and one for the coprecipitated protein (*e.g.* APP in *A*). The *vertical line* in the *lower blot* in *A* indicates that the lanes were on the same gel but not directly next to each other. *IP*, immunoprecipitation with the indicated antibody. *Lysate*, to prove that the transfected cDNAs were expressed, aliquots of the cell lysate were loaded directly and analyzed by immunoblot using the indicated antibody. *sIg7-APLP1 (Y/S)*, Tyr-638 is mutated to Ser.

tested, which carries the cytoplasmic domain of TACE fused to the same sIg7 transmembrane and ectodomain (sIg7-TACE). This protein did not affect APP shedding. All deletion mutants and fusion proteins were expressed in the HEK293 cells as shown by immunoblot analysis in the cell lysate (Fig. 3*B*). Taken together, the domain deletion analysis reveals that the APLP1-induced APP shedding requires the APLP1 cyto-plasmic domain to be membrane-anchored and to be present in a late compartment of the secretory pathway or in the endocytic pathway.

Stimulation of APP Shedding Is Independent of γ-Secretase Activity—Like APP, APLP1 is processed by γ-secretase (9, 10, 12), leading to the release of the cytoplasmic domain, which might translocate to the nucleus and stimulate the transcription of target genes, potentially
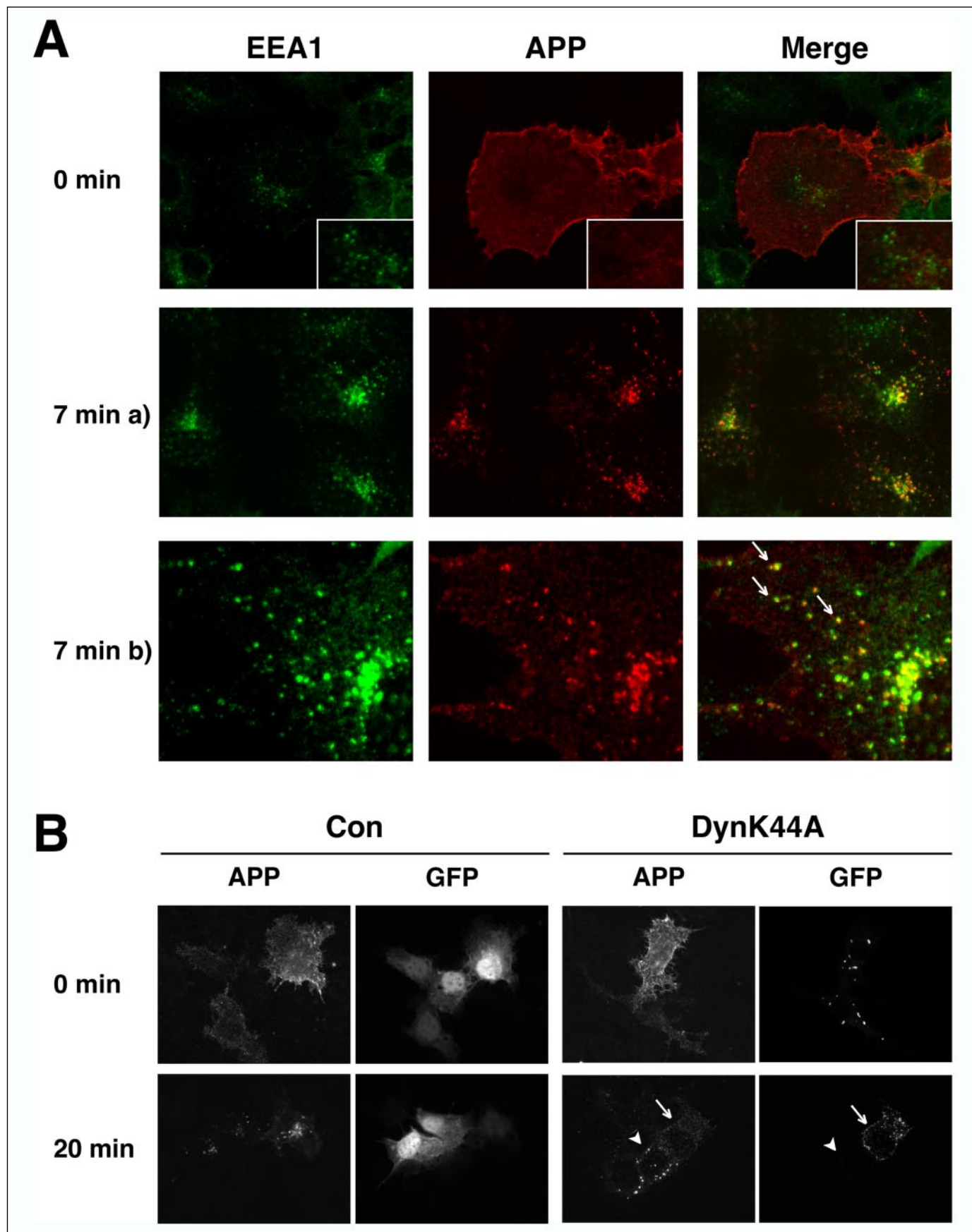
FIGURE 7. **APP antibody uptake assay.** *A*, COS cells were transiently transfected with APP. As described under "Experimental Procedures," cells were incubated on ice with the polyclonal antibody 5313 against the extracellular domain of APP. After the indicated time periods at 37 °C, cells were fixed, permeabilized and stained with a monoclonal anti-EEA1 antibody followed by fluorescently labeled secondary antibodies. Cells were analyzed by confocal microscopy. *Left panels*, EEA1-positive compartments are shown in *green*. *Middle*

including genes involved in APP shedding or endocytosis. If this process is required for the APLP1 effect, an inhibition of γ-secretase activity should reduce the increase in APP shedding observed upon APLP1 transfection. To test this possibility, HEK293 cells were transiently transfected with APLP1 or control vector and then treated with or without the well characterized γ-secretase inhibitor DAPT. Endogenous APP in the cell lysate and in the conditioned medium was detected by immunoblotting using antibody W02. Transfection of APLP1 stimulated APP shedding (Fig. 4*A*, *lanes* 5 and 6) compared with control transfected cells (*lanes 1* and *2*), consistent with the effect seen in Fig. 2. Addition of the γ-secretase inhibitor DAPT had no effect on APP shedding, neither in the control nor in the APLP1-transfected cells. Thus, γ-secretase activity is not required for the APLP1-induced increase in APP shedding. This fits with the experiment in Fig. 3*A* showing that expression of the soluble intracellular domain of APLP1, which corresponds to the γ-secretase-cleaved APLP1 intracellular domain, had no effect on APP shedding. To ensure that DAPT was active, the APLP1 C-terminal fragments were immunoprecipitated from the cell lysates (Fig. 4*B*). In agreement with a previous publication (10), the γ-secretase inhibitor DAPT increased the amount of APLP1 C-terminal fragments.

APLP1 Requires Its Cytoplasmic GYENPTY Motif for the Induction of APP Shedding—To dissect further the molecular mechanism by which the cytoplasmic domain of APLP1 stimulates APP shedding, an additional APLP1 deletion mutant was tested, which lacks the amino acid motif GYENPTY in its cytoplasmic domain. This motif belongs to the NP*XY* class of endocytic trafficking signals (7). It is conserved in the APP homologs and is required for the endocytosis of the APP gene family (33, 34), presumably by providing a binding site for cytoplasmic adapter proteins that may link APP to the endocytic machinery and the clathrin-coated pits. Additionally, this sequence binds cytoplasmic adapter proteins, such as FE65, Dab, and X11, which have been shown to modulate the proteolytic processing of APP (for a review, see Ref. 15). Transient transfection into the AP-APP reporter cell line revealed that APLP1 lacking this motif (APLP1ΔNPTY) has largely lost its ability to induce APP shedding compared with full-length wild-type APLP1 (Fig. 5*A*). A similar result was obtained in a second assay system. In HEK293 cells expressing endogenous wild-type APP, APLP1ΔNPTY caused only a mild increase in APP shedding compared with full-length APLP1 (data not shown). Together, these experiments show that the APLP1-induced increase in APP shedding largely depends on the presence of the GYENPTY motif. Similar NP*XY* endocytosis motifs are found in a small number of unrelated type I membrane proteins, such as members of the LDL receptor family, the insulin receptor (IR) and the EGF receptor (EGFR). Thus, we tested whether other proteins containing an NP*XY* motif also increased APP shedding or whether this effect was specific for APLP1 and the APP family members. In contrast to APLP1, transient transfection of the IR and the EGFR or of LRP-CT had no effect on APP shedding (Fig. 5*B*). Likewise, L-selectin, which lacks an NP*XY* signal and was used as a negative control, did not alter APP shedding. All proteins were expressed as analyzed by immunoblotting (Fig. 5*C*).

The NP*XY* sequence in APLP1 differs from the corresponding sequence in the IR and EGFR in that it is two amino acids C-terminal to a tyrosine (Tyr-682 with respect to APP695 nomenclature, Fig. 5*D*). A

previous study showed that in addition to the NP*XY* motif Tyr-682 is required for efficient endocytosis of APP (34). Thus, we tested whether Tyr-638 in APLP1 (corresponding to Tyr-682 in APP) is required for inducing APP shedding. We used the sIg7-APLP1 construct and replaced Tyr-638 with the amino acid serine (sIg7-APLP1 Y/S), which is found at the corresponding position in the sequence of the IR (Fig. 5*D*). Both constructs were transiently transfected into the AP-APP cells. In contrast to wild-type sIg7-APLP1, which strongly activated APP shedding (Fig. 5*E*; see also Fig. 3*A*), the mutant sIg7-APLP1 Y/S carrying the Y638S mutation had a much weaker effect on APP shedding (Fig. 5*E*), revealing the requirement of Tyr-638 for full activation of APP shedding.

Tyr-682 of APP, in addition to the NPTY motif, is also required for efficient binding of APP to FE65 (35). Therefore, we tested whether the APP shedding-inducing effect of APLP1 correlated with its binding to FE65. Upon transient cotransfection into HEK293 cells, wild-type APP and APLP1 coimmunoprecipitated as expected with FE65 (Fig. 6, *A* and *B*). APLP1 lacking the GYENPTY motif (APLP1ΔNPTY) did not interact with FE65 (Fig. 6*B*), revealing the importance of this motif as the FE65 binding site of APLP1. Moreover, sIg7-APLP1 coimmunoprecipitated with FE65, whereas sIg7-APLP1 Y/S showed a clear reduction of interaction with FE65 (Fig. 6*C*). This shows that, similar to APP, not only the NP*XY* motif, but also the first tyrosine within the GYENPTY motif is necessary for binding to FE65. Neither the insulin receptor (Fig. 6*D*) nor the EGFR (35) interacted with FE65. Taken together, these experiments demonstrate that the APLP1-induced APP shedding correlates with the capability of APLP1 to bind to FE65.

APLP1 Inhibits APP Endocytosis—The requirement for the presence of the endocytic GYENPTY motif in APLP1 suggests the possibility that expression of APLP1 interferes with the rate of APP endocytosis, potentially by inhibiting the binding of APP to FE65 or other endocytic proteins. As a result, more APP would be available for α-secretase cleavage, which is assumed to occur at or close to the plasma membrane (36).

To test for a possible influence of APLP1 on APP endocytosis, an immunofluorescence-based APP antibody uptake assay was used, similar to those described previously (31, 37). In this assay COS cells were transiently transfected with APP. Cell surface APP was labeled by incubating cells on ice with an antibody against the ectodomain of APP. Cells were returned to 37 °C for different incubation times (0, 7, 20, and 35 min) and then fixed, permeabilized, and stained with a fluorescently labeled secondary antibody against the prebound anti-APP antibody. In this assay, using a confocal microscope, APP showed a typical cell surface staining at 0 min (patchy cell surface staining and bright rim of the cell, Fig. 7*A*). As expected, no costaining with the endosomal marker EEA1 is seen at this time point (Fig. 7*A*). At 7 min, numerous cells showed APP-containing vesicles that are EEA1-positive (Fig. 7*A*, *second row* and magnified cell in the *third row*), identifying them as endosomes and showing that APP endocytosis can be visualized in this assay. As a control the COS cells were transiently cotransfected with APP and either GFP as a control or C-terminally GFP-tagged dynamin1 K44A. This dynamin1 mutant is a dominant-negative inhibitor of endocytosis, including the endocytosis of APP (38). As expected, both the GFP-transfected control cells as well as the dynamin K44A-transfected cells

panels, Red shows localization of APP. *Right panels*, merge of EEA1 and APP localization. Colocalization is indicated by *yellow* areas. *7 min a)* and *b),* different cells are shown from the 7 min time point with *7b)* showing a magnification of the cells to visualize colocalization in vesicles. *B*, COS cells were transiently cotransfected with APP and either GFP as a control (*Con*) or the C-terminally GFP-tagged dominant-negative dynamin mutant DynK44A. The antibody uptake assay was carried out as above. Cells were analyzed by standard fluorescence microscopy at the indicated time points. *First* and *third panels*, fluorescence of APP. *Second* and *fourth panels*, fluorescence of GFP or APLP1-GFP. *Upper panel*, At time point 0 min all cells show patchy cell surface staining. Additionally, the rim of the cells shows bright fluorescence. *Lower panel*, after 20 min most GFP-expressing cells show APP endocytosis; DynK44A-GFP expressing cells still show cell surface staining of APP. Note that after 20 min APP cell surface staining is less bright because some cell surface APP has undergone ectodomain shedding.
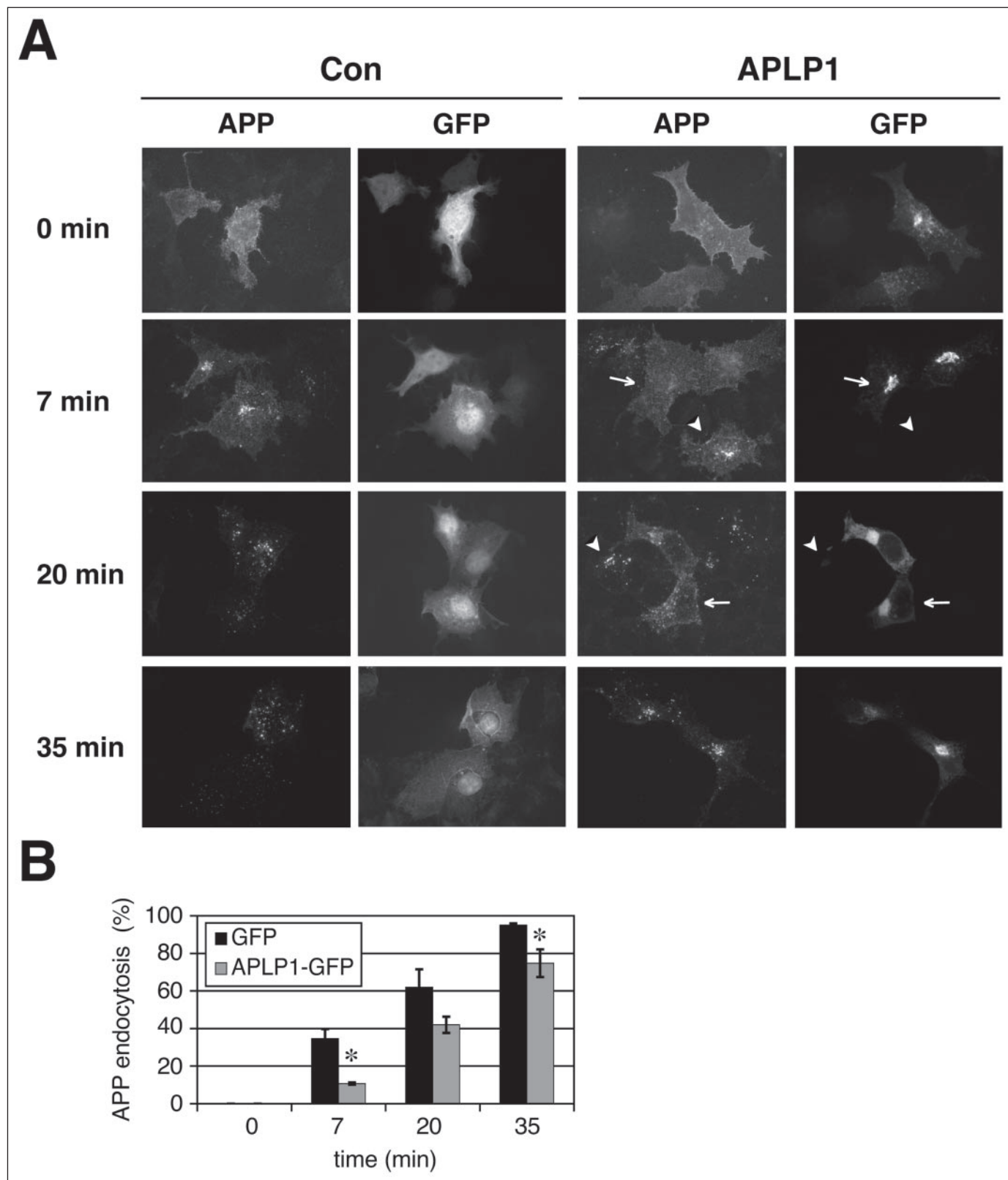
FIGURE 8. **APLP1 reduces the rate of APP uptake.** COS cells were transiently cotransfected with APP and either GFP as a control or C-terminally GFP tagged APLP1. Cells were incubated on ice with the primary antibody 5313 against the extracellular domain of APP. After the indicated time periods at 37 °C cells were fixed, permeabilized, and stained with a fluorescently labeled secondary antibody against the anti-APP antibody. Control (*Con*) and APLP1-transfected cells were analyzed by standard fluorescence microscopy at four different time points. *A*, *first* and *third columns*, fluorescence of APP. *Second* and *fourth columns*, fluorescence of GFP or APLP1-GFP. *Top row*, at time point 0 all cells showed patchy cell surface staining of APP. *Second* to *fourth rows*, APLP1-GFP-expressing cells showed reduced levels of APP endocytosis compared with GFP-expressing cells at all time points analyzed. *Arrows* point to cells that express APLP1. *Arrowheads* point to cells from the same transient transfection, which showed APP expression but no detectable APLP1 expression; these cells showed endocytosis similar to the control cells. Note that at 20 min the cell with the *arrow* has just started undergoing APP endocytosis (APP-positive vesicles and additionally remaining APP cell surface staining can be seen) and looks more like a control cell at the earlier time point of 7 min than like the control cells at 20 min. In contrast, the cell with the

showed APP cell surface staining at time point 0 min (Fig. 7*B*) using a standard fluorescence microscope. After 20 min the GFP control cells showed the typical endosomal APP staining (Fig. 7*B*), indicating that APP endocytosis had occurred. In contrast, the dynamin K44A-transfected cells showed no APP endocytosis at this time point (Fig. 7*B*, *lower row*, *arrow*). In this transient transfection experiment, some cells expressed only one of the two transfected constructs. Importantly, cells that expressed APP but no dynamin K44A clearly showed endosomal APP staining (Fig. 7*B*, *lower row*, *arrowhead*), similar to the control transfected cells.

Having validated the APP endocytosis assay, we next tested for a possible influence of APLP1 on APP endocytosis. To this aim, COS cells were transiently cotransfected with APP and either GFP as a control or C-terminally GFP-tagged APLP1. Using standard fluorescence microscopy analysis the transfected cells were identified by their green fluorescence (GFP or APLP1-GFP) and scored as either showing endocytosis (endocytic APP-positive vesicles, Fig. 8*A*) or not showing endocytosis (patchy cell surface APP staining and no endocytic vesicles, Fig. 8*A*). Because not all cells start endocytosis at the same time, around 100 cells at every time point were analyzed and scored. Representative pictures for every time point are shown in Fig. 8*A*. The statistical analysis in Fig. 8*B* reveals that APP endocytosis occurred in a time-dependent manner in both the APLP1 and the control transfected cells. At time point 0 min none of the APLP1 or control transfected cells showed endocytosis (Fig. 8*B*), as seen with the typical cell surface staining of APP (Fig. 8*A*). At 7 min, about one-third of the control cells (34%) had endocytosed APP, whereas this was the case for only 11% of the APLP1-transfected cells, indicating that APLP1 expression lowered the rate of APP endocytosis. Importantly, cells that expressed APP but not APLP1-GFP (Fig. 8*A*, *arrowhead*) showed normal APP endocytosis similar to the control cells. At 20 min and at 35 min APP endocytosis increased in the control and the APLP1-transfected cells. At 35 min essentially all control cells displayed APP endocytosis. Even most of the APLP1-transfected cells showed endocytosis at this time point, but to a slightly and significantly reduced extent (Fig. 8*B*). This reveals that, unlike dynamin K44A, APLP1 expression does not completely inhibit APP endocytosis, but slows down the rate of APP endocytosis, particularly at the early time point (7 min). As in the dynamin K44A experiment, some cells expressed only APP, but not the GFP-tagged APLP1 (Fig. 8*A*, indicated with *arrowheads* at 7 and 20 min). Similar to the control transfected cells, these cells showed endosomal APP staining, whereas at the same time point the APLP1-expressing cells still showed cell surface APP staining (at 7 min, *arrows*) or only started to show APP endocytosis (at 20 min, *arrows*).

APLP1 Induces APP Shedding in an LRP-dependent Manner—The rate of APP endocytosis and shedding has been shown to depend on the presence of the LRP (21, 22), which is assumed to bind to APP through the adapter protein FE65. In the absence of LRP (knock-out cells) APP endocytosis is impaired, and shedding by α-secretase is increased, similar to what we observed upon expression of APLP1. Thus, we tested whether APLP1 stimulated APP shedding in an LRP-dependent manner. To this aim, CHO cells expressing endogenous wild-type LRP (LRP+/+) or CHO cells lacking LRP expression (LRP−/−) were transiently transfected with APLP1, APLP1ΔNPTY, or empty control vector (Fig. 9*A*). Compared with control transfected cells, APLP1 but not APLP1ΔNPTY, increased endogenous APP shedding in the wild-type

CHO cells by ∼3.5-fold (Fig. 9*A*), similar to the effect seen in HEK293 cells (Fig. 2). Vector transfected LRP−/− cells showed an increased APP secretion compared with the LRP+/+ wild-type cells (data not shown), in agreement with previous publications (21, 22, 24). In these cells, APP secretion has not yet reached its maximum because it can be further enhanced, for example by phorbol 12-myristate 13-acetate (24). However, APLP1 did not further increase APP secretion in the LRP−/− cells significantly (Fig. 9*A*), indicating that in wild-type cells the APLP1-induced increase in APP shedding might be dependent on the LRP-mediated uptake of APP. Importantly, the APLP1-induced increase in APP shedding could be restored in LRP−/− cells that were cotransfected with LRP-CT (Fig. 9*B*).

DISCUSSION

Ectodomain shedding of APP, and more specifically the α-secretase cleavage, can be activated by a variety of different proteins and extracellular stimuli (for a review, see Ref. 6). However, the underlying molecular pathways and mechanisms remain little understood. In this study we identified the APP homolog APLP1 as a novel activator of APP shedding. We show that expression of APLP1 interferes with APP endocytosis, thus making more APP available for an increased shedding at the cell surface. This fits well with previous studies showing that a reduction of wild-type APP endocytosis increases the amount of APP shedding (33, 38). Further support for the involvement of endocytosis in the APLP1-induced APP shedding comes from the results of the domain deletion analysis of APLP1. As expected for a protein that interferes with APP endocytosis, the C-terminal fragment of APLP1 induced APP shedding only when its cytoplasmic domain was membrane-associated and when it was allowed to exit the endoplasmic reticulum. Another result that agrees well with the APLP1-induced reduction of APP endocytosis, is the finding that APLP1 strongly activated the α-secretase cleavage of APP and slightly reduced β-secretase cleavage. The α-secretase is assumed to be active at the cell surface (36), whereas β-cleavage of wild-type APP occurs after endocytosis in the endosomes. For example, APP lacking its cytoplasmic domain including its NPTY internalization motif undergoes much less APP endocytosis and β-secretase cleavage, but more α-secretase cleavage compared with full-length APP (33, 34). Likewise, inhibition of general dynamin-dependent endocytosis, including the inhibition of APP endocytosis, resulted in more endogenous APP at the cell surface and in an increased shedding, mainly by α-secretase and to a lower extent by β-secretase (38).

What is the mechanism underlying the APLP1-induced inhibition of APP endocytosis? APP has been shown to bind to a variety of cytoplasmic adapter proteins, such as FE65, X11, Numb, Shc, mDab, JIP, Grb2, and Abl (for an overview, see Ref. 14), which all seem to compete for the same binding site at or around the NPTY motif in the cytoplasmic domain of APP. Among these proteins, FE65, X11, and JIP have been shown to alter APP trafficking and shedding in cultured cells (see for example 22, 24, 39–44). FE65 and X11 also affect APP processing *in vivo* (45, 46). For the other interactors similar effects have not been reported. Among the interacting proteins, FE65 and X11 have been studied most intensively and seem to have opposite effects on APP shedding and trafficking, with FE65 increasing and X11 decreasing APP shedding. APLP1 binds to the same cytoplasmic proteins as APP (47–49) and may thus reduce binding of APP to FE65, X11, or one of the other cytosolic interactors. If such a competition for APP binding partners is the basis

---

arrowhead looks like the control cell at the same time point of 20 min. Representative pictures of three independent experiments are shown. *B*, around 100 cells expressing GFP or APLP1-GFP were analyzed at every time point and scored as showing or not showing APP endocytosis. Given are the mean ± S.D. of three independent experiments. Counting of cells was done under double blind conditions. *Asterisk* indicates a statistically significant difference ($p < 0.05$, determined by Student's *t* test) between APLP1- and GFP-transfected cells with regard to the number of cells showing endocytosis.
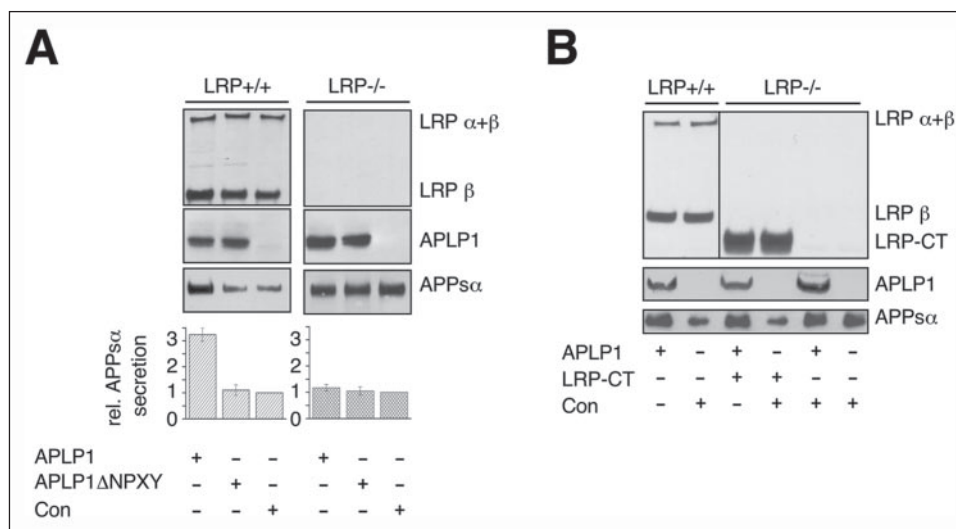
FIGURE 9. **Effect of APLP1 on APP shedding depends on the presence of LRP.** Wild-type CHO cells expressing LRP (LRP+/+) and LRP-deficient CHO cells (LRP−/−) were transiently transfected with control vector (*Con*), with APLP1, APLP1 lacking the cytoplasmic FE65-binding motif (GYENPTY) (*A*) or the LRP-CT (*B*). Aliquots of the conditioned medium and the cell lysates were separated by electrophoresis and blotted for soluble APP in the conditioned medium (antibody 1G75A3) and for LRP (antibody LRP1704) and APLP1 (antibody 57) expression in the cell lysate. *A, lower panel*, quantification of three different experiments, each performed in duplicate. Note that APP secretion is only increased after APLP1 transfection in cells expressing LRP (LRP+/+). *B*, LRP+/+ and LRP−/− cells were transiently transfected with control vector or with APLP1. In addition, LRP−/− cells were cotransfected with APLP1 and LRP-CT. Experiments were performed as described in *A*. Transfection of LRP-CT into LRP−/− cells rescues the effect of APLP1 expression on APP shedding.

for the APLP1-induced phenotype (increase in APP shedding and reduction of APP endocytosis), then this APLP1 phenotype should be similar to a loss-of-function phenotype of the corresponding interactor. Additionally, such an interactor that is bound by APLP1 should affect APP shedding in an LRP-dependent manner because the APLP1-induced APP shedding phenotype was only observed in LRP-expressing cells. Among the interactors of APP and APLP1, FE65 is the best candidate to be involved in the APLP1 phenotype. The RNA interference-mediated knock-down of FE65 in mouse embryonic fibroblasts results in a phenotype that is essentially identical to the APLP1-induced phenotype: increase of APP α-shedding in an LRP-dependent manner. A specific mechanism of how FE65 controls the endocytosis and shedding of APP, but not of unrelated membrane proteins, has been put forward by several groups using different experimental approaches (23–25, 50). According to this model LRP, FE65, and APP form a complex in which the cytosolic FE65 links the cytoplasmic domains of the type I membrane proteins APP and LRP (Fig. 10*A*). In fact, similar to the knock-down of FE65 a knock-out or knock-down of LRP led to increased APP α-shedding (21, 22, 24) (Fig. 10*B*).

One essential aspect of the APP·FE65·LRP model has not yet been tested experimentally. Based on the model we predict that not only a reduction in LRP or FE65 expression should interfere with complex formation, but also the increased expression of membrane proteins that may functionally replace APP in terms of complex formation with FE65 and LRP. Such proteins would compete with APP for the binding to FE65 and LRP (Fig. 10*C*), resulting in a pool of APP, which (*a*) is not complexed to LRP, (*b*) is not efficiently endocytosed, and (*c*) undergoes increased α-secretase cleavage. In agreement with the prediction of the model, not only APLP1 but also APLP2 and the C-terminal C99 fragment of APP increased APP shedding. Even APP itself stimulated APP shedding, which was observed when wild-type APP was transfected into AP-APP cells, where the secretion of the AP-tagged APP (expressed at low levels similar to the endogenous APP (32)) could be clearly separated from the secretion of the untagged wild-type APP. Thus, interfering with APP binding to FE65 and LRP results in a phenotype similar to that in LRP-deficient cells (Fig. 10*C*). This model may also explain why

APLP1 did not induce APP shedding in APP-overexpressing cells. In such cells APP shedding is not only increased, because much more substrate is available for the secretases, but presumably also because not all of the transfected APP forms a complex with the limited amounts of endogenous LRP and FE65. Thus, transfection of APLP1 may not further compete with APP for LRP·FE65 complexes and enhance APP shedding to an extent that can be detected by immunoblot analysis.

In further support of the model, the effect of APLP1 required the cytoplasmic GYENPTY signal, which we identified to be the binding site of FE65. Moreover, the APLP1-induced APP shedding phenotype was not observed in LRP-deficient cells, where the complex cannot form, and APP shedding is already elevated compared with LRP-expressing control cells (Fig. 10*B*). In contrast to the APP gene family, IR, the EGFR, and a membrane-bound LRP-CT had no effect on APP shedding. All three proteins contain one or two cytoplasmic NP*XY* motifs. However, the IR (this study) and the EGFR (35) do not bind FE65 and thus cannot compete with APP for complex formation. In contrast, LRP-CT, which binds FE65 (24), is able to substitute for full-length LRP in the complex, but not for APP, and thus explains the lack of an effect of LRP-CT on APP shedding. Taken together, these experiments provide an additional and essential validation for the model of APP·FE65·LRP complexes in the control of APP shedding and trafficking.

Interestingly, a homolog of LRP, LRP1B, may form a complex with APP similar to LRP itself. A recent study showed that LRP1B can also be coimmunoprecipitated with APP (51), but it remains unclear whether this interaction is also mediated by FE65. In contrast to LRP, which is rapidly endocytosed and mediates efficient APP endocytosis, LRP1B is very slowly endocytosed and reduces APP endocytosis. These experiments reinforce the notion that LRP is an endocytic receptor for APP and that the rate of LRP or LRP1B endocytosis determines the rate of APP endocytosis.

As described above APP and APLP1 bind more cytoplasmic interactors than just FE65/LRP. Such additional interactors could potentially also be involved in the APLP1-induced APP shedding phenotype, but evidence for this is currently lacking. Besides FE65 there is only one more interactor, X11, for which detailed effects on APP shedding have
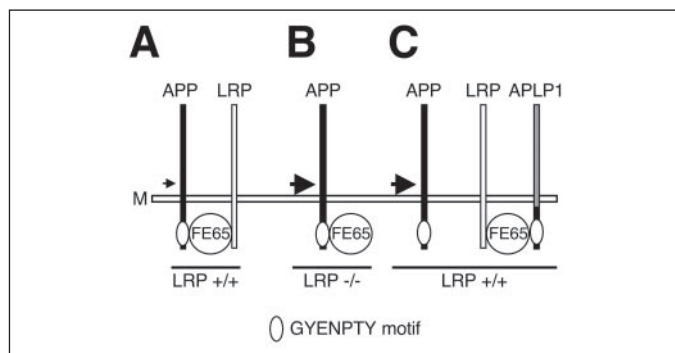
FIGURE 10. **Model for the influence of LRP and APLP1 on APP shedding.** *A*, under wild-type conditions APP, FE65, and LRP form a complex, allowing efficient APP endocytosis and resulting in low levels of APP shedding (*thin arrow*). The size of proteins is not drawn to scale. *B*, in LRP-deficient cells (LRP−/−), endocytosis of APP is reduced, and APP shedding is increased (*bold arrow*). *C*, in cells transfected with APLP1, LRP preferentially forms a complex with APLP1, resulting in APP not being complexed to LRP. This results in a state resembling LRP deficiency (*B*) and an increase in APP shedding (*bold arrow*).

been investigated. Both overexpression and knock-down of X11 lead to an inhibition but not to a stimulation of different aspects of APP processing (43, 46, 52), which is in contrast to the APLP1-induced shedding increase, making a specific involvement of X11 unlikely. For most other APP interactors it is not clear whether and how they influence APP shedding.

In summary, our study reveals a novel and previously unrecognized molecular mechanism for APP shedding, namely that proteins, which substitute for APP in forming complexes with FE65 and LRP, can alter APP shedding. This mechanism is highly specific to the APP gene family. Given that all three proteins of this family can stimulate the shedding of APP, it seems possible that they can also influence the shedding of APLP1 and APLP2. This raises the possibility that changes in the individual expression levels of the three proteins may influence the shedding of all three family members. In fact, expression levels of APP, APLP1, and APLP2 are regulated differentially upon physiological and pathophysiological stimuli in tissue culture and *in vivo*, such as during embryonic development, neuronal differentiation, wound repair, and exposure to the curry spice curcumin, which is currently tested as a treatment option for Alzheimer disease (53–55). Such conditions and stimuli may alter endocytosis and secretion of APP and thus may allow modulating the secretion of the neurotrophic and neuroprotective APPsα and of the pathogenic Aβ peptide.

REFERENCES
1. Hooper, N. M., Karran, E. H., and Turner, A. J. (1997) *Biochem. J.* **321,** 265–279
2. Blobel, C. P. (2000) *Curr. Opin. Cell Biol.* **12,** 606–612
3. Selkoe, D. J., and Schenk, D. (2003) *Annu. Rev. Pharmacol. Toxicol.* **43,** 545–584
4. Citron, M. (2004) *Trends Pharmacol. Sci.* **25,** 92–97
5. Haass, C. (2004) *EMBO J.* **23,** 483–488
6. Allinson, T. M., Parkin, E. T., Turner, A. J., and Hooper, N. M. (2003) *J. Neurosci. Res.* **74,** 342–352
7. Bonifacino, J. S., and Traub, L. M. (2003) *Annu. Rev. Biochem.* **72,** 395–447
8. Bayer, T. A., Cappai, R., Masters, C. L., Beyreuther, K., and Multhaup, G. (1999) *Mol. Psychiatry* **4,** 524–528
9. Scheinfeld, M. H., Ghersi, E., Laky, K., Fowlkes, B. J., and D'Adamio, L. (2002) *J. Biol. Chem.* **277,** 44195–44201
10. Eggert, S., Paliga, K., Soba, P., Evin, G., Masters, C. L., Weidemann, A., and Beyreuther, K. (2004) *J. Biol. Chem.* **279,** 18146–18156
11. Li, Q., and Sudhof, T. C. (2004) *J. Biol. Chem.* **279,** 10542–10550
12. Walsh, D. M., Fadeeva, J. V., LaVoie, M. J., Paliga, K., Eggert, S., Kimberly, W. T., Wasco, W., and Selkoe, D. J. (2003) *Biochemistry* **42,** 6664–6673
13. Bayer, T. A., Paliga, K., Weggen, S., Wiestler, O. D., Beyreuther, K., and Multhaup, G. (1997) *Acta Neuropathol.* **94,** 519–524
14. Russo, C., Venezia, V., Repetto, E., Nizzari, M., Violani, E., Carlo, P., and Schettini, G. (2005) *Brain Res. Brain Res. Rev.* **48,** 257–264
15. King, G. D., and Scott Turner, R. (2004) *Exp. Neurol.* **185,** 208–219
16. Sabo, S. L., Ikin, A. F., Buxbaum, J. D., and Greengard, P. (2003) *J. Neurosci.* **23,** 5407–5415
17. Sabo, S. L., Ikin, A. F., Buxbaum, J. D., and Greengard, P. (2001) *J. Cell Biol.* **153,** 1403–1414
18. Cao, X., and Sudhof, T. C. (2001) *Science* **293,** 115–120
19. Cao, X., and Sudhof, T. C. (2004) *J. Biol. Chem.* **279,** 24601–24611
20. Herz, J., and Strickland, D. K. (2001) *J. Clin. Invest.* **108,** 779–784
21. Ulery, P. G., Beers, J., Mikhailenko, I., Tanzi, R. E., Rebeck, G. W., Hyman, B. T., and Strickland, D. K. (2000) *J. Biol. Chem.* **275,** 7410–7415
22. Pietrzik, C. U., Busse, T., Merriam, D. E., Weggen, S., and Koo, E. H. (2002) *EMBO J.* **21,** 5691–5700
23. Kinoshita, A., Whelan, C. M., Smith, C. J., Mikhailenko, I., Rebeck, G. W., Strickland, D. K., and Hyman, B. T. (2001) *J. Neurosci.* **21,** 8354–8361
24. Pietrzik, C. U., Yoon, I. S., Jaeger, S., Busse, T., Weggen, S., and Koo, E. H. (2004) *J. Neurosci.* **24,** 4259–4265
25. Trommsdorff, M., Borg, J. P., Margolis, B., and Herz, J. (1998) *J. Biol. Chem.* **273,** 33556–33560
26. Steiner, H., Kostka, M., Romig, H., Basset, G., Pesold, B., Hardy, J., Capell, A., Meyn, L., Grim, M. L., Baumeister, R., Fechteler, K., and Haass, C. (2000) *Nat. Cell Biol.* **2,** 848–851
27. Seubert, P., Oltersdorf, T., Lee, M. G., Barbour, R., Blomquist, C., Davis, D. L., Bryant, K., Fritz, L. C., Galasko, D., and Thal, L. J. (1993) *Nature* **361,** 260–263
28. Ida, N., Hartmann, T., Pantel, J., Schröder, J., Zerfass, R., Förstl, H., Sandbrink, R., Masters, C. L., and Beyreuther, K. (1996) *J. Biol. Chem.* **271,** 22908–22914
29. Lichtenthaler, S. F., Dominguez, D. I., Westmeyer, G. G., Reiss, K., Haass, C., Saftig, P., De Strooper, B., and Seed, B. (2003) *J. Biol. Chem.* **278,** 48713–48719
30. Dovey, H. F., John, V., Anderson, J. P., Chen, L. Z., de Saint Andrieu, P., Fang, L. Y., Freedman, S. B., Folmer, B., Goldbach, E., Holsztynska, E. J., Hu, K. L., Johnson-Wood, K. L., Kennedy, S. L., Kholodenko, D., Knops, J. E., Latimer, L. H., Lee, M., Liao, Z., Lieburg, I. M., Motter, R. N., Mutter, L. C., Nietz, J., Quinn, K. P., Sacchi, K. L., Seubert, P. A., Shopp, G. M., Thorsett, E. D., Tung, J. S., Wu, J., Yang, S., Yin, C. T., Schenk, D. B., May, P. C., Altstiel, L. D., Bender, M. H., Boggs, L. N., Britton, T. C., Clemens, J. C., Czilli, D. L., Dieckman-McGinty, D. K., Droste, J. J., Fuson, K. S., Gitter, B. D., Hyslop, P. A., Johnstone, E. M., Li, W. Y., Little, S. P., Mabry, T. E., Miller, F. D., and Audia, J. E. (2001) *J. Neurochem.* **76,** 173–181
31. Kaether, C., Lammich, S., Edbauer, D., Ertl, M., Rietdorf, J., Capell, A., Steiner, H., and Haass, C. (2002) *J. Cell Biol.* **158,** 551–561
32. Ting, A., Lichtenthaler, S., Xavier, R., Na, S. Y., Rabizadeh, S., Holmes, T., and Seed, B. (2005) *Novartis Found. Symp.* **267,** 219–230
33. Koo, E. H., and Squazzo, S. L. (1994) *J. Biol. Chem.* **269,** 17386–17389
34. Perez, R. G., Soriano, S., Hayes, J. D., Ostaszewski, B., Xia, W., Selkoe, D. J., Chen, X., Stokin, G. B., and Koo, E. H. (1999) *J. Biol. Chem.* **274,** 18851–18856
35. Borg, J. P., Ooi, J., Levy, E., and Margolis, B. (1996) *Mol. Cell. Biol.* **16,** 6229–6241
36. Sisodia, S. S. (1992) *Proc. Natl. Acad. Sci. U. S. A.* **89,** 6075–6079
37. Haass, C., Koo, E. H., Mellon, A., Hung, A. Y., and Selkoe, D. J. (1992) *Nature* **357,** 500–503
38. Chyung, J. H., and Selkoe, D. J. (2003) *J. Biol. Chem* **278,** 51035–51043
39. Lee, J. H., Lau, K. F., Perkinton, M. S., Standen, C. L., Rogelj, B., Falinska, A., McLoughlin, D. M., and Miller, C. C. (2004) *J. Biol. Chem.* **279,** 49099–49104
40. Sabo, S. L., Lanier, L. M., Ikin, A. F., Khorkova, O., Sahasrabudhe, S., Greengard, P., and Buxbaum, J. D. (1999) *J. Biol. Chem.* **274,** 7952–7957
41. Sastre, M., Turner, R. S., and Levy, E. (1998) *J. Biol. Chem.* **273,** 22351–22357
42. Guenette, S. Y., Chen, J., Ferland, A., Haass, C., Capell, A., and Tanzi, R. E. (1999) *J. Neurochem.* **73,** 985–993
43. Borg, J. P., Yang, Y., De Taddeo-Borg, M., Margolis, B., and Turner, R. S. (1998) *J. Biol. Chem.* **273,** 14761–14766
44. Taru, H., Kirino, Y., and Suzuki, T. (2002) *J. Biol. Chem.* **277,** 27567–27574
45. Santiard-Baron, D., Langui, D., Delehedde, M., Delatour, B., Schombert, B., Touchet, N., Tremp, G., Paul, M. F., Blanchard, V., Sergeant, N., Delacourte, A., Duyckaerts, C., Pradier, L., and Mercken, L. (2005) *J. Neurochem.* **93,** 330–338
46. Xie, Z., Romano, D. M., and Tanzi, R. E. (2005) *J. Biol. Chem.* **280,** 15413–15421
47. Homayouni, R., Rice, D. S., Sheldon, M., and Curran, T. (1999) *J. Neurosci.* **19,** 7507–7515
48. Bressler, S. L., Gray, M. D., Sopher, B. L., Hu, Q., Hearn, M. G., Pham, D. G., Dinulos, M. B., Fukuchi, K., Sisodia, S. S., Miller, M. A., Disteche, C. M., and Martin, G. M. (1996) *Hum. Mol. Genet.* **5,** 1589–1598
49. Duilio, A., Faraonio, R., Minopoli, G., Zambrano, N., and Russo, T. (1998) *Biochem. J.*

330, 513–519

50. Rebeck, G. W., Moir, R. D., Mui, S., Strickland, D. K., Tanzi, R. E., and Hyman, B. T. (2001) *Brain Res. Mol. Brain Res.* **87,** 238–245

51. Cam, J. A., Zerbinatti, C. V., Knisely, J. M., Hecimovic, S., Li, Y., and Bu, G. (2004) *J. Biol. Chem.* **279,** 29639–29646

52. Araki, Y., Tomita, S., Yamaguchi, H., Miyagi, N., Sumioka, A., Kirino, Y., and Suzuki, T. (2003) *J. Biol. Chem.* **278,** 49448–49458

53. Beckman, M., and Iverfeldt, K. (1997) *Neurosci. Lett* **221,** 73–76

54. Kummer, C., Wehner, S., Quast, T., Werner, S., and Herzog, V. (2002) *Exp. Cell Res.* **280,** 222–232

55. Adlerz, L., Beckman, M., Holback, S., Tehranian, R., Cortes Toro, V., and Iverfeldt, K. (2003) *Brain Res. Mol. Brain Res.* **119,** 62–72